Shape-invariant pulses in resonant linear absorbers

Soodeh Haghgoo* and Sergey A. Ponomarenko

Department of Electrical and Computer Engineering, Dalhousie University, Halifax, NS, B3J 2X4 Canada
**Corresponding author: soodeh@dal.ca*

Received December 1, 2011; revised February 13, 2012; accepted February 23, 2012;
posted February 24, 2012 (Doc. ID 159214); published April 6, 2012

We theoretically describe ultrashort self-similar pulses propagating in coherent linear absorbers near optical resonance and propose a method for their experimental realization.
OCIS codes: 030.0030, 320.0320, 320.5550.

Shape-invariant light beams enjoy a special place in optics due to their self-similar structure on paraxial propagation in free space. Several classes of shape-invariant fully and partially coherent beams, including, notably, Hermite–Gaussian (HG) ones, are known so far [1,2]. Owing to the space–time duality between evolution of beams in free space and pulses in optical fibers [3], similar shape-invariant pulses exist in weakly dispersive media far away from internal resonances.

Close to an optical resonance, however, one may expect to see, in general, pronounced pulse reshaping due to enhanced dispersion there [4]. Yet, we have shown elsewhere [5] that shape-invariant pulses emerge as universal intermediate asymptotics on near-resonant pulse propagation in coherent *linear amplifiers* as a result of dynamical balance between amplification and dissipation processes. Since no such balance is feasible in *linear absorbers*, the prospects for self-similarity there are open to debate.

In this Letter, we show that a broad class of shape-invariant ultrashort pulses is nevertheless supported by resonant linear absorbers. We stress that self-similarity arises here thanks to a particular class of initial spectral profiles with long wings where much of the incident pulse energy is stored. We also discuss the potential for experimental realization of the new pulses in homogeneously broadened coherent absorbers and estimate the necessary pulse and optical media parameters.

We start by examining small-area pulse propagation in a homogeneously broadened resonant absorber under the exact resonance condition: the pulse carrier frequency coincides with a resonant transition frequency of the medium atoms. An atomic vapor in the homogeneously broadening regime [1], filling the core of a hollow-core photonic crystal fiber (HCPCF) [6] can serve as a physical realization of the medium. Using the HCPCF, we can arrest spatial diffraction. Engineering the fiber to tune its zero group-velocity dispersion frequency to the gas resonance frequency enables us to eliminate bulk medium dispersion effects and focus on purely resonant properties of the system.

In the slowly varying envelope approximation (SVEA), the pulse field $\mathcal{E}(z,t)$ and atomic dipole moment $\sigma(z,t)$ can be shown to obey the classical Maxwell–Lorentz equations [5,7]:

$$\partial_\zeta \Omega = i\kappa\sigma, \tag{1}$$

$$\partial_\tau \sigma = -\gamma_\perp \sigma + i\Omega, \tag{2}$$

which are written in the transformed variables: $\zeta = z$ and $\tau = t - z/c$. Here we also introduced the field envelope in frequency units, $\Omega = -e\mathcal{E}/2m\omega x_0$, where x_0 is an amplitude of the electron displacement from equilibrium, the inverse dipole relaxation rate $\gamma_\perp = 1/T_\perp$, where $T_\perp$ is a characteristic dipole moment relaxation time, and a coupling constant, $\kappa = Ne^2/4\epsilon_0 mc$. The coupled Maxwell–Lorentz equations, Eqs. (1) and (2), can be solved using a Fourier transform technique, yielding the field envelope at any propagation distance in the form

$$\mathcal{E}(\tau,\zeta) = \int_{-\infty}^{\infty} \mathrm{d}\nu \tilde{\mathcal{E}}_0(\nu) e^{-i\nu\tau} \exp\left[-\frac{\alpha\zeta}{2(1-i\nu T_\perp)}\right]. \tag{3}$$

Here, $\alpha = 2\kappa/\gamma_\perp$ is a small-signal absorption coefficient and we introduce the spectral amplitude of the incident pulse by the expression

$$\tilde{\mathcal{E}}_0(\nu) = \int_{-\infty}^{\infty} \frac{\mathrm{d}t}{2\pi} \mathcal{E}(t,0) e^{i\nu t}. \tag{4}$$

With an eye on shape-invariant pulse evolution, we consider the following family of incident pulses:

$$\mathcal{E}_s(t,0) = \mathcal{E}_{0s}\theta(t)(\kappa\zeta_0 t)^{s/2} J_s\left(2\sqrt{\kappa\zeta_0 t}\right) e^{-\gamma_\perp t}, \tag{5}$$

where s is a nonnegative real mode index and $\theta(t)$ is a unit step function, mathematically describing a physical zero-index pulse with a very short rise time t_r. As was discussed in detail in the amplifier context in [5], the inequality $\omega^{-1} \ll t_r \ll T_\perp$ must be respected for the SVEA to work.

Using the integral representation [8]

$$\int_0^\infty \mathrm{d}x x^{s+1} e^{-a^2x^2} J_s(bx) = \frac{b^s}{(2a^2)^{s+1}} e^{-b^2/4a^2}, \tag{6}$$

and changing the variable of integration, we can obtain the pulse spectral amplitude in the source plane as

$$\tilde{\mathcal{E}}_{0s}(\nu) = \frac{\tilde{\mathcal{E}}_{ms}}{(1-i\nu T_\perp)^{s+1}} \exp\left[-\frac{\alpha\zeta_0}{2}\left(\frac{i\nu T_\perp}{1-i\nu T_\perp}\right)\right]. \tag{7}$$

Here we introduce the peak spectral amplitude $\tilde{\mathcal{E}}_{ms}$ as

$$\tilde{\mathcal{E}}_{ms} = \frac{\mathcal{E}_{0s} T_\perp}{2\pi} \left(\frac{\alpha\zeta_0}{2}\right)^s e^{-\alpha\zeta_0/2}, \tag{8}$$

which links ζ_0 to the other pulse parameters. Next, on comparing the Fourier decomposition of the incident pulse,

$$\mathcal{E}_s(t,0) = \int_{-\infty}^{\infty} d\nu \tilde{\mathcal{E}}_{s0}(\nu) e^{-i\nu t}, \tag{9}$$

with that at any $\zeta \geq 0$—see Eq. (3)—and using Eq. (7), we infer by inspection that the examined pulse [Eq. (5)] indeed remains self-similar on propagation in the resonant medium with the pulse profile given by

$$\mathcal{E}_s(\tau,\zeta) = \frac{\mathcal{E}_{0s}\theta(\tau)}{(1+\zeta/\zeta_0)^s} \eta^{s/2} J_s\left(2\sqrt{\eta}\right) e^{-\gamma_\perp \tau}. \tag{10}$$

Here, the similarity variable η is defined as $\eta = \kappa(\zeta+\zeta_0)\tau$. Hereafter, we will refer to $\{\mathcal{E}_s\}$ as a set of resonant linear absorber modes. Note that the new mode index s need not be an integer, which sets the discovered modes apart from, for instance, familiar HG ones encountered in the laser resonator theory [1].

Next, over sufficiently long propagation distances, $\zeta \gg \zeta_0$, the pulse shape is independent of its initial rms width, $\mathcal{E}_s(\tau,\zeta) \propto \theta(\tau)(\kappa\tau/\zeta)^{s/2} J_s(2\sqrt{\kappa\zeta\tau}) e^{-\gamma_\perp \tau}$. Hence, the rms width of the pulse must be independent of ζ_0 in the long-term limit as well, a feature that further distinguishes novel modes from the HG ones. The rms pulse width of the zero-index mode is exhibited in Fig. 1 as a function of the propagation distance for different initial conditions in the dimensionless variables: $T = \tau/T_\perp$, $Z = \alpha\zeta$, and $Z_0 = \alpha\zeta_0$.

It follows at once from Eqs. (3) and (7) that the spectrum of the shape-invariant pulse of index s can be represented as

$$S_s(\omega, Z) = \frac{S_0}{(1+\omega^2)^{s+1}} \exp\left(-\frac{Z+Z_0}{1+\omega^2}\right). \tag{11}$$

The spectral profile of the zero-index mode is shown in Fig. 2—the other mode spectra look qualitatively similar—as a function of dimensionless frequency $\omega = \nu T_\perp$ for $Z_0 = 0.5$ and $Z_0 = 7$. As is seen in the figure, the spectrum evolution scenario is determined by the interplay of resonant dispersion and absorption and it strongly depends on the magnitude of Z_0. For sufficiently small Z_0—see Fig. 2(a)—the initial spectrum has a central peak. A hole is then burnt at the center of the pulse spectrum on propagation over a fraction of a characteristic absorption length. This is followed by spectral hole broadening as the energy is being steadily transferred toward the pulse wings and the pulse evolution becomes self-similar. A source with a greater Z_0 may already have a spectral hole–as is illustrated in Fig. 2(b)—resulting in shape-invariant pulse propagation from the outset. To exhibit self-similarity in the time domain, we also display the zero-mode pulse evolution in the insets in Fig. 2.

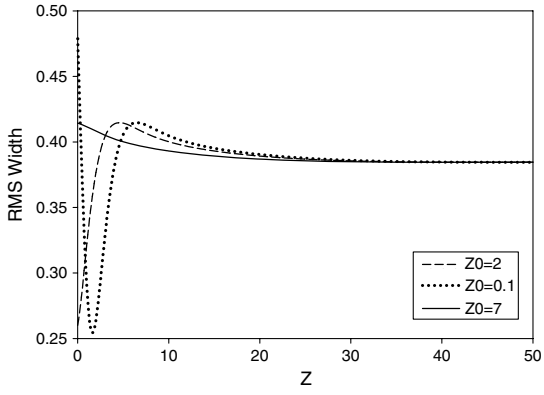

Fig. 1. Root-mean-square width of the zero-index pulse as a function of Z for three values of Z_0.

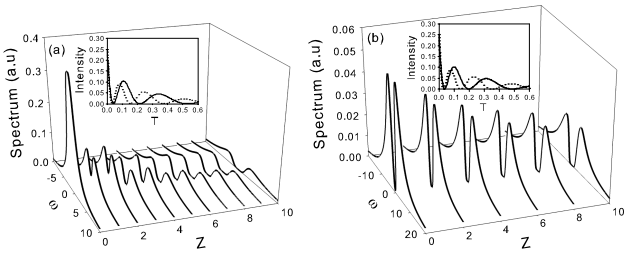

Fig. 2. Pulse spectrum of the zero-index mode (in arbitrary units) as a function of dimensionless frequency ω and propagation distance Z for (a) $Z_0 = 0.5$ and (b) $Z_0 = 7$. Insets: zero-index pulse intensity profile as a function of dimensionless time T; $Z = 70$, (dotted curve) and $Z = 100$ (solid curve).

The required pulse profile to generate self-similarity can be synthesized by exploring Eq. (7). It follows from Eq. (7) that the desired spectral shape consists of an atomic absorption profile—the Lorentzian prefactor–and a complex modulation factor, $H(\nu) = (1+\nu^2 T_\perp^2)^{-s} \exp[-\alpha\zeta_0/(1-i\nu T_\perp)]$. The amplitude and phase of the latter are sketched in Fig. 3 as functions of ω.

Next, to generate the overall spectrum, one may first invert an atomic ensemble in a source gas cell with an ultrashort π pulse, say. The excited atoms will then emit a homogeneously broadened pulse of Lorentzian spectral shape, which may, in turn, be spectrally filtered with the filter function $H(\nu)$ using, for example, one of the techniques reviewed in [9].

Further, we briefly discuss the required material parameters to realize the discussed pulses. First, the collision-induced spectral width $\delta\nu_c$—assuming dipole relaxation is mainly due to collisions, $T_\perp \sim \delta\nu_c^{-1}$—must be much greater than the Doppler-induced inhomogeneous broadening width $\delta\nu_D$. To attain the homogeneous broadening

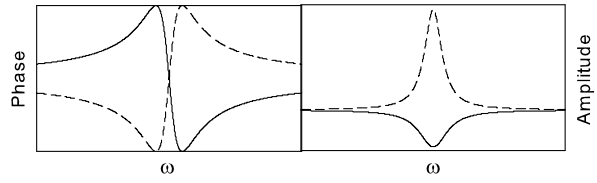

Fig. 3. Left: the filter phase (solid) and the real part of the refractive index (dashed). Right: the filter amplitude (solid) and the imaginary part of the refractive index (dashed).

regime, $\delta\nu_c \gg \delta\nu_D$, one can either collimate the gas beam or increase the gas pressure [1]. Taking the gas density to be $N \sim 10^{15}$ cm^{-3}—which is, at least, 3 orders of magnitude beyond the usual dilute vapor range [7]—and assuming $T_\perp \sim 10^{-12}$ s for such a dense vapor, we estimate the linear absorption length $L_A = \alpha^{-1} \simeq 0.2$ mm. Thus, the self-similar pulse propagation regime can be observable in a few-meters-long HCPCF.

Finally, let us estimate the required input pulse energy density, $W = (\epsilon_0 c/2)\int_{-\infty}^{\infty} \mathrm{d}t|\mathcal{E}|^2 = \pi\epsilon_0 c \int_{-\infty}^{\infty} \mathrm{d}\nu|\tilde{\mathcal{E}}|^2$. Using the peak spectral amplitude of the input pulse, the energy density can be roughly estimated as $\tilde{\mathcal{E}}_{ms}^2 \Delta\nu$, where the spectral width (FWHM) is $\Delta\nu \sim T_\perp^{-1}$. The peak spectral amplitude can, in turn, be estimated using the pulse area, $\mathcal{A} = (2d/\hbar)\int_{-\infty}^{\infty} \mathrm{d}t\mathcal{E} = 2\pi\tilde{\mathcal{E}}_m$. In the small-area regime, say, $\mathcal{A} \sim 0.1$, we arrive at $W \simeq 10$ nJ/cm^2, where we used $d \sim ea_0 \sim 10^{-29}$ C m as a reasonably good estimate for the dipole moment magnitude in optical transitions [7]. Thus, the proposed self-similar pulses can be realized with picosecond pulse sources of just 10 nJ/cm^2 energy.

References

1. P. W. Milonni and J. H. Eberly, *Lasers* (Wiley, 1985).
2. F. Gori, Opt. Commun. **34**, 301 (1980).
3. J. Lancis, V. Torres-Company, E. Silvestre, and P. Andrés, Opt. Lett. **30**, 2973 (2005).
4. M. D. Crisp, Phys. Rev. A **6**, 2001 (1972).
5. S. Haghgoo and S. A. Ponomarenko, Opt. Express **19**, 9750 (2011).
6. P. St. J. Russell, J. Lightwave Technol. **24**, 4729 (2006).
7. L. Allen and J. H. Eberly, *Optical Resonance and Two-Level Atoms* (Dover, 1975).
8. M. Abramowitz and I. A. Stegan, *Handbook of Mathematical Functions* (Dover, 1972).
9. C. Froehly, B. Colombeau, and M. Vampouille, in *Progress in Optics*, E. Wolf, ed. (1981), Vol. 20, pp. 115–135.